Journal Name

ARTICLE

Hybrid conjugated polymers with alternating dithienosilole or dithienogermole and tricoordinate boron units

Received 00th January 20xx,
Accepted 00th January 20xx

DOI: 10.1039/x0xx00000x

www.rsc.org/

Yohei Adachi,[a] Yousuke Ooyama,[a] Yi Ren,[b] Xiaodong Yin,[b] Frieder Jäkle,[b]* and Joji Ohshita[a]*

Conjugated polymers composed of tricoordinate boron and π-conjugated units possess extended conjugation with low-lying LUMOs arising from p_B-π interactions. However, donor-acceptor (D-A) polymers that feature triorganoboranes alternating with highly electron-rich donors remain scarce. We present here a new class of hybrid D-A polymers that combine electron-rich dithienosiloles or dithienogermoles with highly robust tricoordinate borane acceptors. Polymers of high molecular weight are readily prepared by Pd-catalyzed Stille coupling reaction of bis(halothienyl)boranes and distannyldithienosiloles or -germoles. The polymers are obtained as dark red solids that are stable in air and soluble in common organic solvents. Long wavelength UV-vis absorptions at ca. 500-550 nm indicate effective π-conjugation and pronounced D-A interactions along the backbone. The emission maxima occur at wavelengths longer than 600 nm in solution and experience further shifts to lower energy with increasing solvent polarity, indicative of strong intramolecular charge transfer (ICT) character of the excited state. The powerful acceptor character of the borane comonomers is also evident from cyclic voltammetry (CV) analyses that reveal low-lying LUMO levels of the polymers. Density functional theory (DFT) calculations on model oligomers further support these experimental observations.

Introduction

There has been growing interest in donor-acceptor (D-A) type π-conjugated polymers in the field of organic materials. Intramolecular electronic interactions between the donor and acceptor units give rise to extended conjugation, resulting in low band gap polymers. Intermolecular through-space interactions in the solid state are also enhanced, which facilitates the hopping carrier mobility between polymer chains. Because of these intriguing optoelectronic properties, applications of conjugated D-A polymers as active materials in organic optoelectronic devices, such as organic photovoltaics (OPVs) and organic field-effect transistors (OFETs), have been widely explored.[1-8] For use in electronic devices, controlling the electronic states of the polymers is of critical importance to precisely match those of other materials in the devices. Thus, many types of electron donor and acceptor fragments with different electronic states have been developed. However, they are usually based on common π-conjugated units and strategies that introduce new building blocks are highly anticipated. One approach that has attracted much recent attention involves the development of new conjugated building blocks that feature electron-rich or electron-deficient main group elements, allowing for effective tuning of the electronic structure.[9-11]

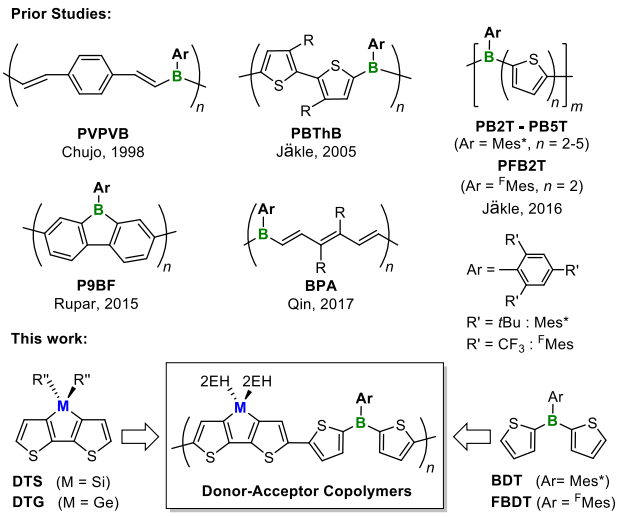

Chart 1 Examples of electron-deficient tricoordinate organoboron polymers and targeted organoborane-dithienosiloles/dithienogermoles D-A polymers.

Among different main group elements, boron stands out in that when introduced into π-conjugated systems it dramatically alters the electronic states.[12-19] Interactions between the boron vacant p-orbital and π*-orbitals effectively lower the LUMO level of an organic conjugated π-system. In pioneering work, the group of Naka and Chujo demonstrated the formation of divinylbenzene-borane alternating polymers **PVPVB** (Chart 1) by the

[a] Department of Applied Chemistry, Graduate School of Engineering, Hiroshima University, Higashi-Hiroshima 739-8527, Japan. Tel: +81-82-424-7743. Fax: +81-82-424-5494. E-mail: jo@hiroshima-u.ac.jp.
[b] Department of Chemistry, Rutgers University Newark, 73 Warren Street, Newark, New Jersey 07102, United States. E-mail: fjaekle@rutgers.edu.

Electronic Supplementary Information (ESI) available: [Characterization details including NMR and mass spectra, DSC curves, absorption spectra, fluorescence spectra, and anodic cyclic voltammograms]. See DOI: 10.1039/x0xx00000x

hydroboration of diethynylbenzene and mesitylborane as the first example of tricoordinate boron-containing conjugated polymers.[12] Following this original finding, several other routes to boron-containing conjugated polymers (e.g., **PBThB**, **P9BF**, **BPA**) have been introduced, resulting in a range of new materials with intriguing electronic and optical properties.[20-28] However, a drawback is that many of these polymers show limited stability in ambient atmosphere because of the high reactivity of the tricoordinate boron centers towards oxygen and moisture. Recently, some of us introduced the highly air-stable tricoordinate thienylboranes **BDT** and **FBDT** (Chart 1) as robust and versatile building blocks of conjugated polymers.[29] In these structures, the central boron atom is protected by the bulky Mes* (2,4,6-tris(*tert*-butyl)phenyl) or ^{F}Mes (2,4,6-tris(trifluoromethyl)phenyl) group, making it possible to handle them without special care. In addition to the steric protection, the fluorine-containing ^{F}Mes group greatly enhances the electron-accepting properties of the tricoordinate boron in the p_B-π system.[30] Polythiophenes with tricoordinate boron embedded in the main chain were readily prepared via Stille cross coupling (**PB2T-PB5T**, **PFB2T** in Chart 1).[31] These polymers exhibit intriguing properties, such as red-shifted UV-vis absorptions, derived from the extended conjugation through the p-orbital on boron, and strong emission in solution as well as the film state.[31] However, donor-acceptor polymers that combine robust tricoordinate organoborane moieties and highly electron-rich donors in their backbone remain exceedingly rare.[32,33]

We introduce here a new class of hybrid donor-acceptor polymers that incorporate both strongly electron-accepting tricoordinate borane units (BDT, FBDT) and highly electron-rich dithienosilole (DTS) and dithienogermole (DTG) donor units (Chart 1). The electron-rich planar tricyclic π-systems of DTS and DTG give rise to strong emission and enhanced conjugation compared with 2,2'-bithiophene itself. They have been widely used as efficient donor units of conjugated D-A oligomers and polymers for organic electronic device materials, such as OPVs,[34-45] OFETs,[46-49] dye-sensitized solar cells,[50-57] and organic light-emitting diodes.[58-64] However, they have not yet been explored as comonomers of boron-containing conjugated polymers. We report here the first examples of polymers containing both tricoordinate boron and electron-rich silole/germole moieties in the backbone. These polymers exhibit pronounced intramolecular charge transfer (ICT) character as indicated by low energy absorptions and strong solvatochromic effects in the photoluminescence spectra. The experimental observations are discussed together with the results of quantum chemical calculations on molecular model compounds.

Results and discussion

Synthesis

The DTS/DTG-containing organoborane polymers were prepared as presented in Scheme 1. **BDTI2** was synthesized as reported in the literature[29] and the organoborane monomer **FBDTBr2** was prepared by the Sn-B exchange reaction of BBr_3 with 2 equivalents of (5-bromothien-2-yl)trimethylstannane,

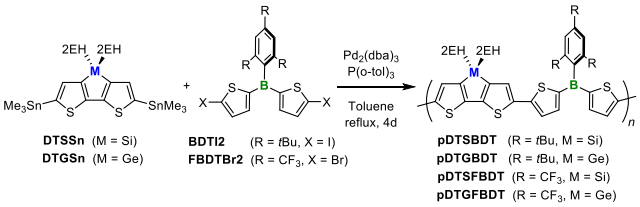

Scheme 1 Synthesis of hybrid borane-dithienosilole/germole copolymers.

followed by the reaction of the resulting intermediate, bis(5-bromothien-2-yl)bromoborane with 2,4,6-tris(trifluoromethyl)phenyllithium. The NMR and mass spectra of the intermediate and monomer **FBDTBr2** are available in the Supporting Information (Fig. S1-S7). To obtain polymers with sufficient solubility, we introduced branched 2-ethylhexyl groups on the Si and Ge bridging atoms. The Stille cross-coupling reactions of bis(2,6-trimethylstannyl)dithienoheteroles and bis(5-halothienyl)boranes were examined under the conditions similar to those reported for other D-A polymers containing group 14 element bridged bithiophene units.[43,65] The reactions proceeded smoothly in refluxing toluene. The resulting solutions containing the polymers were passed through a short silica gel column with chlorobenzene as eluent to remove the Pd catalyst. Polymers **pDTSBDT** and **pDTGBDT** were further purified by reprecipitation from toluene/ethanol and then from toluene/acetone, whereas **pDTSFBDT** and **pDTGFBDT** were reprecipitated twice from chloroform/ethanol. All the polymers were stable in air and well soluble in common organic solvents, such as hexane, toluene, chloroform, and THF.

The polymer structures were verified by NMR and MALDI-TOF MS analysis (Fig. S8-S22). ^{11}B NMR measurements at room temperature gave no clear signals, but spectral data acquired at 50 °C revealed broad peaks around 45 ppm (Fig. S12), which is in a similar range as for the corresponding organoboron monomers.[29,31] The presence of the ^{F}Mes substituents on boron in **pDTSFBDT** and **pDTGFBDT** was further confirmed by sharp singlets due to the *ortho*- and *para*-CF_3 groups (-58.4, -65.2 ppm) in the ^{19}F NMR spectra (Fig. S17). For **pDTSBDT** and **pDTSFBDT**, the ^{29}Si NMR spectra displayed only one major resonance (-5.4, -5.1 ppm), consistent with incorporation of the silole moieties into the polymers (Fig. S18). Thus, the heteronuclear NMR data clearly confirm the integrity of the building blocks in the polymer structures. In the ^{1}H NMR spectra of the polymers peaks were observed at reasonable chemical shifts and with nearly ideal integral ratios (Fig. S8-S11). For instance, the aromatic protons of the ^{F}Mes groups appear at a characteristic chemical shift of 8.18 ppm, while those of the Mes* groups resonate at 7.45 ppm. ^{13}C NMR measurements were also performed for all the polymers at 50 °C, providing spectra that are well resolved, even revealing the C-F coupling for the ^{F}Mes-substituted polymers (Fig. S13-S16). The number of signals and chemical shifts of the major peaks were consistent with the expected structures. Small additional peaks of very low intensity in the aromatic region are tentatively attributed to polymer end groups.

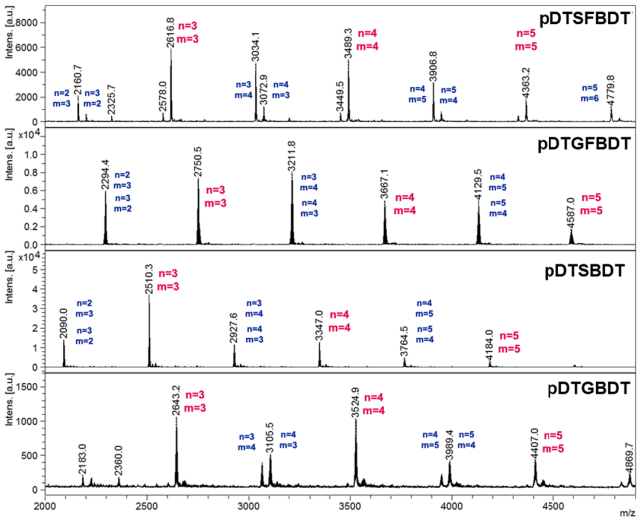

Fig. 1 Section of the MALDI-TOF MS of hybrid borane-dithienosilol/dithienogermole copolymers (positive mode, matrix: trans-2-[3-(4-tert-butylphenyl)-2-methyl-2-propenylidene]malononitrile).

To further elucidate the microstructure of the polymers, MALDI-TOF mass spectra were acquired. Series with peak spacings that match well with the repeating units consisting of a DTS/DTG (n) and borane (m) unit were readily identified. As illustrated in Fig. 1, oligomers are detected with up to ca. n, m = 5 units for each building block. Both types of terminal groups are present as suggested by peak series corresponding to n = m, n = m+1, and n = m-1 for the number of constituting building blocks. Surprisingly, matching of the peak distributions to calculated peak patterns indicated the absence of additional protons at the chain ends (Fig. S19-S22). This may suggest that cyclic species are formed, at least in case of the relatively low molecular weight species that are detectable by MALDI-TOF MS. For some of the samples relatively much smaller peaks corresponding to oligomers with an additional DTS or DTG moiety are also detected (n = m+2, Fig. S19-S20). This is most pronounced for **pDTGFBDT**, but almost completely absent in the spectra of **pDTSBDT** and **pDTGBDT**, and indicates the presence of a homo-coupled unit. Consistent is that in the ^{1}H NMR spectra we found a small peak at around 7.1 ppm (Fig. S8-S11), which is similar in chemical shift to DTS/DTG homopolymers.[37,43] The ratios of the homo-coupled units to the desired ideal alternating structure, however, is very small, estimated to be approximately 10 % based on ^{1}H NMR integral ratios both for **pDTSBDT** and **pDTGBDT** and less than 5% for the fluorinated polymers.

Table 1 Data for hybrid borane-dithienosilol/dithienogermole copolymers.

Polymer	Yield /% [a]	M_n [b]	Đ [b]	T_d^5 [c] /°C
pDTSBDT	53	9,400	1.9	308
pDTGBDT	52	12,400	2.0	308
pDTSFBDT	83	13,900	4.2	406
pDTGFBDT	78	15,300	3.6	403

[a] Reprecipitated from toluene/ethanol and then from toluene/acetone (**pDTSBDT**, **pDTGBD**) or twice from toluene/ethanol (**pDTSFBDT**, **pDTGFBDT**). [b] Determined by GPC analysis ($Đ = M_w/M_n$). [c] 5% weight loss temperatures determined by thermogravimetric analysis (TGA) in nitrogen.

The molecular weights of the polymers were estimated by gel permeation chromatography (GPC) using polystyrene standards (Table 1). Polymers **pDTSBDT** and **pDTGBDT** showed monomodal GPC profiles with dispersities (Đ) of 1.9 and 2.0, respectively, whereas bimodal distributions with larger dispersities were found for **pDTSFBDT** and **pDTGFBDT**. We also carried out thermogravimetric analysis (TGA) of the polymers to evaluate their thermal stability. The temperatures corresponding to 5% weight loss (T_d^5) were noted at 308 °C for both **pDTSBDT** and **pDTGBDT** in nitrogen. These values are comparable to those of previously reported polymers such as **PB4T** (Chart 1).[31] Notably, the T_d^5 values of **pDTSFBDT** and **pDTGFBDT** are over 400 °C and comparable to those of homopolymers of DTS (T_d^5 = 414 °C, M_n = 42,000)[43] and DTG (T_d^5 = 400 °C, M_n = 33,000).[38] This difference is likely ascribable to the higher thermal stability of the CF_3 in comparison to the *t*Bu groups. We also performed differential scanning calorimetry (DSC) analyses to determine the melting and glass transition points of the polymers in nitrogen. For **pDTSBDT** and **pDTGBDT** no transitions could be observed from room temperature to 250 °C, but the scans for **pDTSFBDT** and **pDTGFBDT** displayed glass transition points at 107 °C and 127 °C in the second scan (Fig. S23 and S24).

Photophysical properties

The photophysical properties of the polymers are summarized in Tables 2 and 3. In addition, representative absorption and fluorescence spectra of the borane-dithienogermole copolymers in solution and in the film state are displayed in Fig. 2 and those of the corresponding borane-dithienosilole copolymers are illustrated in Fig. S25 and S26. The absorption maxima of all polymers (λ_{max}^{abs} in the range of 532 to 562 nm in THF) are red-shifted with respect to those of the borane building blocks **BDT** (λ_{max}^{abs} = 324 nm in THF) and **FBDT** (λ_{max} = 326 nm in THF)[29] and unsubstituted quaterthiophene (λ_{max}^{abs} = 393 nm in CH_2Cl_2),[66] indicating that the conjugation is effectively extended due to p_B-π interactions. Importantly, the absorption maxima are also significantly red-shifted from that of thiophene copolymer **PB4T** (Chart 1, λ_{max}^{abs} = 480 nm in THF),[31] which contains the same number of thiophene units between tricoordinate boron centers. This result points to a pronounced effect of the electron-rich DTS/DTG donor units. The spectral data of the polymers are very similar regardless of the heterole bridging element (Si or Ge), but the absorption and emission bands of the ^{F}Mes-substituted polymers **pDTSFBDT** and **pDTGFBDT** are further red-shifted relative to those of **pDTSBDT** and **pDTGBDT** containing Mes* substituents on boron. This observation suggests that the D-A interaction between the borane and dithienosilole/germole units strongly depends on the electron-deficient character of boron, which is enhanced for the ^{F}Mes relative to the Mes*-substituted borane moiety. The absorption bands are not significantly affected by the nature of the solvent,

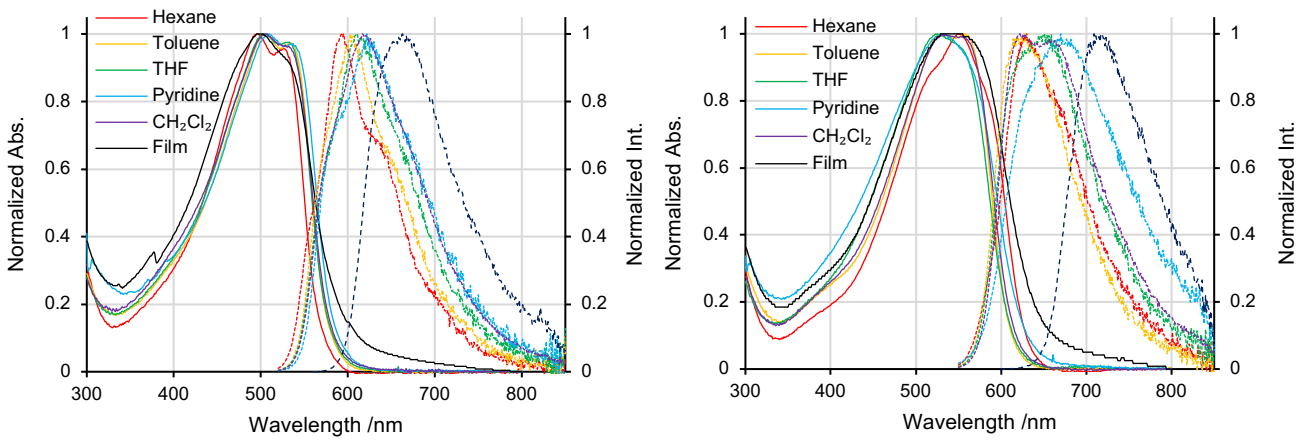

Fig. 2 Absorption (solid lines) and fluorescence (dashed lines) spectra of **pDTGBDT** (left) and **pDTGFBDT** (right) in solution and as thin film.

and in the film state they appear at wavelengths similar to those in solution, indicating rather weak intermolecular interactions in the ground state (Table 2). In contrast, the fluorescence spectra show a strong dependence on the solvent polarity (Table 3). In non-polar solvents intense emissions are observed in the range of 592 to 630 nm with quantum yields from 32-41%. As the solvent polarity increases, the emission maxima (λ_{max}^{em}) are shifted to longer wavelengths and the fluorescence quantum yields (Φ) gradually decrease. This tendency is in line with a pronounced ICT character of the photoexcited states.[67,68] Again, a dramatic bathochromic shift is observed for the ^{F}Mes-borane copolymers relative to the Mes*-borane copolymers, resulting in emission maxima up to 670 nm for **pDTGFBDT** in pyridine as the solvent. We expected the polymers to be also emissive in the film state, because the bulky Mes* and ^{F}Mes substituents should inhibit intermolecular interactions. However, the emission of the polymers in the film state is weak and the fluorescence quantum yields could not be determined reliably (<2%). Moreover, the emission bands were red-shifted from those in solution, signifying strong intermolecular interactions. As the absorption spectra of the polymers are nearly independent of the state (solution or film), the red-shifted emission for the films is likely due to further stabilization of the excited state by intermolecular interaction, such as excimer or exciplex formation. To further explore this aspect, we prepared 0.5wt% PMMA films of **pDTSBDT** and **pDTSFBDT**. The emission maxima of the PMMA-embedded polymer films are clearly blue-shifted from those of the neat films while the quantum yield increases significantly (**pDTSBDT** λ_{max}^{em} = 626 nm, Φ = 2%; **pDTSFBDT** λ_{max}^{em} = 665 nm, Φ = 6%; Fig. S27). This supports the notion that excimer or exciplex formation plays a significant role in the condensed film state.

Electrochemical properties

Table 2 Absorption data of borane-dithienosilole/germole copolymers.

Polymer	λ_{max}^{abs} /nm					
	Hexane [a]	Toluene [a]	THF [a]	Pyridine [a]	CH_2Cl_2 [a]	Film [b]
pDTSBDT	525, 495	535, 504	533, 502	537, 510	533, 505	535[c], 496
pDTGBDT	527, 497	533, 508	532, 505	537, 510	537[c], 507	538[c], 500
pDTSFBDT	548, 515[c]	558, 527	556, 526	525	557, 529	544
pDTGFBDT	550, 517[c]	558, 527	562[c], 523	533	561, 535	540

[a] Carried out in 8.0 mg/L solution. [b] Spin-coated film on quartz glass. [c] Shoulder peak.

Table 3 Fluorescence data of borane-dithienosilole/germole copolymers.

Polymer	λ_{max}^{em} /nm (Φ /%)					
	Hexane [c]	Toluene [c]	THF [c]	Pyridine [c]	CH_2Cl_2 [c]	Film [d]
pDTSBDT [a]	592 (32)	606 (33)	613 (30)	627 (23)	616 (11)	650 (-[e])
pDTGBDT [a]	595 (36)	603 (32)	611 (25)	622 (18)	617 (12)	663 (-[e])
pDTSFBDT [b]	627 (41)	616 (30)	654 (19)	665 (6)	622 (14)	697 (-[e])
pDTGFBDT [b]	630 (36)	629 (29)	651 (17)	670 (4)	622 (15)	709 (-[e])

[a] Excited at 500 nm. [b] Excited at 530 nm. [c] Carried out in 8.0 mg/L solution. [d] Drop-casted film on quartz glass. [e] Too weak to enable determination of quantum yield.

Table 4 Electrochemical data of borane-dithienosilole/germole copolymers.

Polymer	E_{red} [a] /V (Fc/Fc$^+$)	LUMO [b] /eV	E_{ox} [c] /V (Fc/Fc$^+$)	HOMO [d] /eV	E_g(CV) [e] /eV	E_g(Opt) [f] /eV
pDTSBDT	-1.99	-2.81	0.66	-5.46	2.65	2.16
pDTGBDT	-1.98	-2.82	0.63	-5.43	2.61	2.15
pDTSFBDT	-1.75	-3.05	0.67	-5.47	2.42	2.07
pDTGFBDT	-1.74	-3.06	0.64	-5.44	2.38	2.02
PB4T [g]	-1.89	-2.90	-	-	-	2.29

[a] Onset of reductive wave in CV using 0.1 M tetrabutylammonium perchlorate in MeCN as supporting electrolyte and a scan rate of 50 mV s^{-1}. [b] Determined as –(4.8 + E_{red}). [c] Onset of oxidative wave in CV. [d] Determined as –(4.8 – E_{ox}). [e] Determined as E_{ox} – E_{red}. [f] Obtained from the onset of absorption in THF. [g] Reference 31

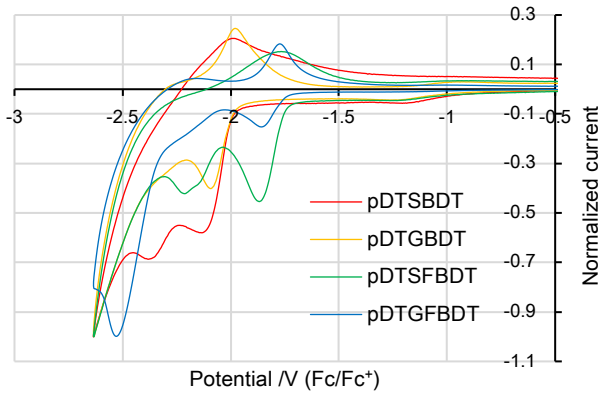

Fig. 3 Cyclic voltammetry data (reductive waves) of borane-dithienosilole/germole copolymers films in acetonitrile with 0.1 M tetrabutylammonium perchlorate as supporting electrolyte at a scan rate of 50 mV s^{-1}.

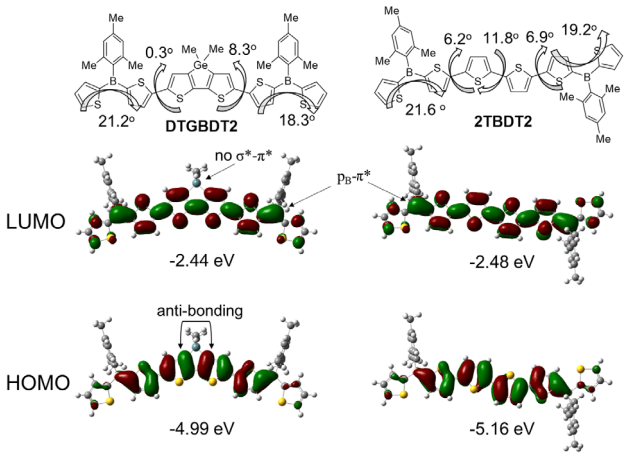

Fig. 4. Frontier orbital depictions of model compounds (B3LYP/6-31G(d,p)).

To further evaluate the electronic structures of the polymers, cyclic voltammetry measurements were performed on the polymer films in acetonitrile containing tetrabutylammonium perchlorate as the supporting electrolyte. The cathodic cyclic voltammograms (CVs) are shown in Fig. 3, revealing pseudo-reversible reductive couples. As borane-quarterthiophene copolymer **PB4T** (Chart 1) solutions revealed reversible cathodic profiles,[31] the modest electrochemical reversibility for the present polymers is likely due to the different experimental conditions (solution vs film) and possibly also associated with cathodic instability of the DTS/DTG units. The LUMO levels as estimated from the onsets of reduction (E_{red}) are significantly lower for **pDTSFBDT** and **pDTGFBDT** in comparison to those of **pDTSBDT** and **pDTGBDT**, reflecting the strong electron-withdrawing ability of the ^{F}Mes group. We also investigated the anodic properties of the polymers. The polymer films gave irreversible anodic peaks and, in contrast to their cathodic behaviors, no clear dependence of the anodic peak potentials on the polymer structures was seen (Fig. S28). On the basis of the CV onset potentials (E_g(CV)), the HOMO-LUMO gaps decrease in the order of **pDTSBDT** > **pDTGBDT** >> **pDTSFBDT** > **pDTGFBDT**, which agrees well with the trend for the optical bandgaps (E_g(Opt)). We further deduce that the narrowed E_g of **pDTSFBDT** and **pDTGFBDT** compared to those of **pDTSBDT** and **pDTGBDT** is primarily due to the lower LUMO levels.

Theoretical studies

To gain further insights into the electronic structures of the present polymers, density functional theory (DFT) calculations were carried on the model compounds **DTGBDT2** and **2TBDT2** at the B3LYP/6-31G(d,p) level of theory on Gaussian 09 program. The *t*Bu and 2-ethylhexyl groups were replaced with methyl groups in the models to simplify the calculations. The frontier orbitals of **DTGBDT2** and **2TBDT2** derived from these calculations are shown in Fig. 4. The two model compounds exhibit very similar HOMO and LUMO orbital distributions regardless of whether a Si/Ge-fused or unfused bithiophene bridge is present. The HOMOs and LUMOs are mainly distributed on the central thiophene rings and the adjacent boron atoms, but the HOMOs are more localized on the quaterthiophene cores. The LUMOs have significant contributions from the boron p-orbitals, indicating effective p_B-π* conjugation. However, σ*-π* conjugation is not evident for the DTG unit. It is known that such a conjugation tends to be suppressed in highly conjugated π-systems.[43,69] The HOMO energy level of **DTGBDT2** is significantly higher than that of **2TBDT2**. This is in part due to the better planarity of **DTGBDT2**, as shown in Fig. 4, but the electron donating effect of the germanium atom in the DTG unit may also contribute to raising the HOMO. It may also be speculated that the bithiophene moiety in the DTG unit is fixed in a *syn* geometry, inducing a through-space anti-bonding interaction between the 3,3'-positions in DTG to raise the HOMO level of **DTGBDT2**. While the higher planarity of **DTGBDT2** might be expected to

also lower the LUMO level due to more effective conjugation, the calculated LUMO energy of **DTGBDT2** is comparable to that of **2TBDT2**. A possible reason is that the electron-donating character of DTG raises not only the HOMO but also the LUMO level.

Conclusions

We have prepared a new class of conjugated hybrid polymers, in which electron-deficient tricoordinate borane moieties are for the first time combined with electron-rich dithienosilole and dithienogermole donor units. The resulting conjugated hybrid polymers are stable under ambient conditions and well soluble in common organic solvents, including hexane, toluene, and THF. Effective D-A interactions are evidenced by strong bathochromic shifts of the absorption and emission maxima and solvatochromic effects in the fluorescence spectra, indicating a pronounced ICT character at the excited state. Emission maxima of up to 700 nm demonstrate the effectiveness of our approach of combining electron-deficient boranes with low-lying LUMO levels and electron-rich dithienosilole /dithienogermole building blocks with high-lying HOMO levels. Our results further suggest potential utility of these new hybrid D-A polymers in fluorescence imaging and optoelectronic applications, such as photovoltaic or non-linear optical materials.

Experimental

General

NMR spectra were recorded on Varian System 500 and 400MR spectrometers. $BF_3{\cdot}Et_2O$ and fluorobenzene were used as the external and internal standards for ^{11}B and ^{19}F NMR measurements, respectively. MALDI-TOF mass spectra were obtained on a Bruker Ultraflextreme instrument in positive mode, using trans-2-[3-(4-*tert*-butylphenyl)-2-methyl-2-propenylidene]malononitrile) as the matrix. Molecular weights of the polymers were determined by gel permeation chromatography (GPC) using THF as eluent and serially connected Shodex KF2001 and KF2002 columns, relative to polystyrene standards. TGA was carried out on an SII TG/DTA-6200 analyzer under gentle nitrogen flow (100 mL/min) at a heating rate of 10 °C/min. DSC data were acquired with an Exstar DSC6200 thermal analyzer (Seiko Instruments). The sample was packed in an aluminum pan and heated at a rate of 10 °C min^{-1} under nitrogen from 25 to 250 °C (**pDTSBDT** and **pDTGBDT**) or 300 °C (**pDTSFBDT** and **pDTGFBDT**), taking the decomposition temperature of the polymers by TGA into account, then cooled to 25 °C at the same rate. This operation was repeated twice and the thermal transitions were derived from the second cycle. UV-vis absorption spectra were measured with a Shimadzu UV-3600 plus spectrometer. Photoluminescence (PL) spectra were measured with HORIBA FluoroMax-4 spectrophotometers. The PL quantum yields were determined by using a HORIBA FluoroMax-4 spectrophotometer attached to an integration sphere. CVs were measured with an AMETEK VersaSTAT 4 potentiostat/galvanostat in a solution of 0.1 M tetrabutylammonium perchlorate (TBAP) in acetonitrile using a three-electrode system with a Pt plate counter electrode, a Pt wire working electrode, and an Ag/Ag^+ reference electrode. The polymer (1 mg) and TBAP (10 mg) were dissolved in 1 mL of chlorobenzene, and the solution was drop-casted on the working electrode and dried under vacuum for 2 h at 50 °C. DFT calculations were performed on a Gaussian 09 program at B3LYP/6-31G(d,p) level of theory. All reactions were carried out under dry argon. The reaction solvents were purchased from Kanto Chemical Co., Ltd. and were distilled from calcium hydride and stored over activated molecular sieves under argon until use. Starting materials, **DTSSn**,[70] **DTGSn**,[35] and **BDTI2**[29] were prepared according to the literature.

Synthesis of FBDTBr2

In a glovebox, to a solution of BBr_3 (0.31 mL, 3.3 mmol) in 5 mL toluene was added a solution of (5-bromothien-2-yl)trimethylstannane (2.1 g, 6.4 mmol) in 5 mL toluene at room temperature. The mixture was stirred overnight at room temperature. The volatile components were then removed under high vacuum. The intermediate was used in the next step without further purification. ^1H NMR (499.9 MHz, δ in $CDCl_3$, 25 °C): 7.90 (d, J = 5.0 Hz, 4H), 7.33 (d, J = 5.0 Hz, 4H). ^{11}B NMR (160.3 MHz, δ in $CDCl_3$, 25 °C) 47.8 ppm. To 1,3,5-tris(trifluoromethyl)benzene (1.48 g, 5.3 mmol) in 100 mL of dry ether, n-BuLi (3.3 mL, 1.6 M in hexane, 5.3 mmol) were added dropwise at -78 °C. The mixture was stirred for another 0.5 h at this temperature, then warmed to room temperature and stirred for 4 h. The solvent was removed under high vacuum to obtain 1-lithio-2,4,6-tris(trifluoromethyl)benzene as a light yellow solid. The solid was suspended in 5 mL toluene and transferred to a solution of the bromoborane intermediate in toluene at room temperature. The reaction mixture was stirred for 24 hours at room temperature. Water was added and the aqueous layer was extracted with DCM (3×10 mL). All solvents were removed via rotary evaporation. The crude product was purified by flash column chromatography using hexanes as eluent. The product is obtained as a light yellow solid (42% yield). ^1H NMR (599.7 MHz, δ in $CDCl_3$, 25 °C): 8.15 (s, 2H), 7.25 (d, J = 4 Hz, 2H, Th), 7.12 (d, J = 4 Hz, 2H, Th). ^{13}C NMR (150.8 MHz, δ in $CDCl_3$, 25 °C): 143.7 (br, C-B), 143.3, 143.3 (br, C-B), 134.8 (q, $J_{C\text{-}F}$ = 32 Hz, *o*-$\underline{C}CF_3$), 132.8, 132.4 (q, $J_{C\text{-}F}$ = 35 Hz, *p*-$\underline{C}CF_3$), 127.2, 126.4 (br, Th), 123.6 (q, $J_{C\text{-}F}$ = 276 Hz, *o*-CF_3), 122.9 (q, $J_{C\text{-}F}$ = 273 Hz, *p*-CF_3). ^{11}B NMR (192.4 MHz, δ in $CDCl_3$, 25 °C): 49.7 ($w_{1/2}$ = 1000 Hz). ^{19}F NMR (470.4 MHz, δ in $CDCl_3$, 25 °C): –56.2 (s), –63.2 (s). HRMS: m/z = 615.8573 ($[M]^-$, calcd for $C_{17}H_5BBr_2F_9S_2$ 615.8204). Elemental analysis calcd (%) for $C_{17}H_6BBr_2F_9S_2$: C 33.15, H 0.98; found: C 33.62, H 0.99.

Polymer Synthesis

A mixture of 225 mg (0.303 mmol) of **DTSSn**, 204 mg (0.303 mmol) of **BDTI2**, 13.9 mg (5 mol%) of $Pd_2(dba)_3$, 18.3 mg (20 mol%) of P(*o*-tol)$_3$, and 10 mL of toluene was heated to reflux for 4 days. The mixture was cooled to room temperature and subjected to short silica gel chromatography with chlorobenzene as the eluent. The eluate was evaporated and the residue was reprecipitated from 3 mL of toluene into 200 mL of EtOH and

then from 3 mL of toluene into 200 mL of acetone to give 133 mg (52% yield) of **pDTSBDT** as a red powder: ^{1}H NMR (400 MHz, δ in $CDCl_3$): 7.58 (br s, 2H, thiophene), 7.45 (s, 2H, Mes*), 7.32 (s, 2H, DTS), 7.26-7.21 (m, 2H, thiophene), 1.51-1.42 (2H, CH in 2EH), 1.40 (s, 9H, CH_3 in Mes*), 1.35-0.92 (m, 20H, CH_2 in 2EH), 1.23 (s, 18H, CH_3 in Mes*), 0.88-0.72 (m, 12H, CH_3 in 2EH). ^{11}B NMR (160.4 MHz, δ in $CDCl_3$, 50 °C): 46.5 ($w_{1/2}$ = 4500 Hz). ^{13}C NMR (125.7 MHz, δ in $CDCl_3$, 50 °C): 151.8 (sp^2), 148.5 (sp^2), 147.7 (sp^2), 146.7 (sp^2), 144.7 (DTS), 142.3 (sp^2), 138.4 (DTS), 134.7 (sp^2), 127.8 (sp^2), 126.2 (sp^2), 124.7 (sp^2), 122.7 (sp^2), 38.7 (*t*Bu), 35.9 (2EH), 35.6 (2EH), 35.0 (*t*Bu), 34.7 (*t*Bu), 31.4 (*t*Bu), 29.0 (2EH), 28.9 (2EH), 23.1 (2EH), 17.7 (2EH), 14.2 (2EH), 10.8 (2EH). ^{29}Si NMR (99.3 MHz, δ in $CDCl_3$, 50 °C): -5.4. TGA: T_d^5 308 °C (in nitrogen). Melting point was not observed up to 250 °C by DSC in nitrogen.

Polymer **pDTGBDT** was prepared from 238 mg (0.301 mmol) of **DTGSn** and 203 mg (0.302 mmol) of **BDTI2** as a red powder (137 mg, 53% yield) in a manner similar to that above. The polymer was purified by reprecipitating from 3 mL of toluene into 200 mL of EtOH and then from 3 mL of toluene into 200 mL of acetone: ^{1}H NMR (400 MHz, δ in $CDCl_3$): 7.58 (br s, 2H, thiophene), 7.45 (s, 2H, Mes*), 7.32 (s, 2H, DTG), 7.26-7.21 (m, 2H, thiophene), 1.60-1.48 (m, 2H, CH in 2EH), 1.40 (s, 9H, CH_3 in Mes*), 1.38-1.12 (m, 20H, CH_2 in 2EH), 1.24 (s, 18H, CH_3 in Mes*), 0.88-0.72 (m, 12H, CH_3 in 2EH). ^{11}B NMR (160.4 MHz, δ in $CDCl_3$, 50 °C): 45.8 ($w_{1/2}$ = 4700 Hz). ^{13}C NMR (125.7 MHz, δ in $CDCl_3$, 50 °C): 151.8 (sp^2), 148.5 (sp^2), 147.5 (sp^2), 146.7 (sp^2), 146.1 (DTG), 142.3 (sp^2), 138.2 (DTG), 134.7 (sp^2), 127.9 (sp^2), 126.2 (sp^2), 124.6 (sp^2), 122.7 (sp^2), 38.7 (*t*Bu), 37.0 (2EH), 35.5 (2EH), 35.0 (*t*Bu), 34.7 (*t*Bu), 31.4 (*t*Bu), 28.9 (2EH), 28.8 (2EH), 23.1 (2EH), 20.8 (2EH), 14.2 (2EH), 10.9 (2EH). TGA: T_d^5 308 °C (in nitrogen). Melting point was not observed up to 250 °C by DSC in nitrogen.

Polymer **pDTSFBDT** was prepared from 235 mg (0.318 mmol) of **DTSSn** and 195 mg (0.317 mmol) of **FBDTBr2** as a purple powder (216 mg, 78% yield) in a manner similar to that above. The polymer was purified by reprecipitating twice from 3 mL of chloroform into 200 mL of EtOH: ^{1}H NMR (400 MHz, δ in $CDCl_3$): 8.18 (s, 2H, ^{F}Mes), 7.54-7.40 (m, 2H, thiophene), 7.35 (br s, 2H, DTS), 7.33-7.28 (m, 2H, thiophene), 1.50-1.38 (m, 2H, CH in 2EH), 1.38-0.92 (m, 20H, CH_2 in 2EH), 0.88-0.74 (12H, CH_3 in 2EH). ^{11}B NMR (160.4 MHz, δ in $CDCl_3$, 50 °C): 44.7 ($w_{1/2}$ = 4000 Hz). ^{13}C NMR (125.7 MHz, δ in $CDCl_3$, 50 °C): 150.1 (sp^2), 149.3 (sp^2), 145.4 (DTS), 145.0 (sp^2), 143.6 (sp^2), 140.6 (sp^2), 138.1 (DTS), 134.9 (q, $J_{C\text{-}F}$ = 32 Hz, *o*-$\underline{C}CF_3$), 131.9 (q, $J_{C\text{-}F}$ = 34 Hz, *p*-$\underline{C}CF_3$), 128.7 (sp^2), 126.1 (sp^2), 125.4 (sp^2), 123.7 (q, $J_{C\text{-}F}$ = 276 Hz, *o*-CF_3), 123.0 (q, $J_{C\text{-}F}$ = 273 Hz, *p*-CF_3), 36.1, 35.9, 29.1, 29.0, 23.0, 18.0, 14.0, 10.8. ^{19}F NMR (470.4 MHz, δ in $CDCl_3$): -58.4 (m), -65.2 (s). ^{29}Si NMR (99.3 MHz, δ in $CDCl_3$, 50 °C): -5.1. TGA: T_d^5 406 °C (in nitrogen). DSC: T_g 107 °C (in nitrogen).

Polymer **pDTGFBDT** was prepared from 250 mg (0.317 mmol) of **DTGSn** and 195 mg (0.317 mmol) of **FBDTBr2** as a purple powder (241 mg, 83% yield) in a manner similar to that above. The polymer was purified by reprecipitating twice from 3 mL of chloroform into 200 mL of EtOH: ^{1}H NMR (400 MHz, δ in $CDCl_3$): 8.18 (s, 2H, ^{F}Mes), 7.54-7.40 (m, 2H, thiophene), 7.35 (br s, 2H, DTG), 7.34-7.28 (m, 2H, thiophene), 1.58-1.45 (m, 2H, CH in 2EH), 1.38-1.10 (m, 20H, CH_2 in 2EH), 0.91-0.77 (12H, CH_3 in 2EH). ^{11}B NMR (160.4 MHz, δ in $CDCl_3$, 50 °C): 46.0 ($w_{1/2}$ = 3900 Hz). ^{13}C NMR (125.7 MHz, δ in $CDCl_3$, 50 °C): 150.1 (sp^2), 146.9 (sp^2), 146.8 (DTG), 145.1 (sp^2), 143.6 (sp^2), 140.5 (sp^2), 137.9 (DTG), 134.9 (q, $J_{C\text{-}F}$ = 32 Hz, *o*-$\underline{C}CF_3$), 131.9 (q, $J_{C\text{-}F}$ = 34 Hz, *p*-$\underline{C}CF_3$), 128.7 (sp^2), 126.0 (sp^2), 125.3 (sp^2), 123.7 (q, $J_{C\text{-}F}$ = 276 Hz, *o*-CF_3), 123.0 (q, $J_{C\text{-}F}$ = 273 Hz, *p*-CF_3), 37.2, 35.7, 29.1, 28.9, 23.1, 21.2, 14.0, 10.9. ^{19}F NMR (470.4 MHz, δ in $CDCl_3$): -58.4 (m), -65.2 (s). TGA: T_d^5 403 °C (in nitrogen). DSC: T_g 127 °C (in nitrogen).

Conflicts of interest

There are no conflicts to declare.

Acknowledgements

This work was supported by JSPS KAKENHI Grant Number JP24102005, JP17H03105. F.J., Y.R. and X.Y. thank the National Science Foundation for support (Grant CHE-1362460). We thank Abdullah Al.Ahmadi and Dr. Roman Brukh for assistance with acquisition of MALDI-TOF mass spectral data.

References

1 S. W. Thomas III, G. D. Joly and T. M. Swager, *Chem. Rev.*, 2007, **107**, 1339–1386.
2 A. C. Grimsdale, K. L. Chan, R. E. Martin, P. G. Jokisz and A. B. Holmes, *Chem. Rev.*, 2009, **109**, 897–1091.
3 A. Facchetti, *Chem. Mater.*, 2011, **23**, 733–758.
4 Y. Li, *Acc. Chem. Res.*, 2012, **45**, 723–733.
5 C. Duan, F. Huang and Y. Cao, *J. Mater. Chem.*, 2012, **22**, 10416–10434.
6 C. Liu, K. Wang, X. Gong and A. J. Heeger, *Chem. Soc. Rev.*, 2016, **45**, 4825–4846.
7 S. Holliday, J. E. Donaghey and I. McCulloch, *Chem. Mater.*, 2014, **26**, 647−663.
8 W. Zhao, S. Li, H. Yao, S. Zhang, Y. Zhang, B. Yang and J. Hou, *J. Am. Chem. Soc.*, 2017, **139**, 7148–7151.
9 X. M. He and T. Baumgartner, *RSC Adv.*, 2013, **3**, 11334–11350.
10 A. M. Priegert, B. W. Rawe, S. C. Serin and D. P. Gates, *Chem. Soc. Rev.*, 2016, **45**, 922–953.
11 S. M. Parke, M. P. Boone and E. Rivard, *Chem. Commun.*, 2016, **52**, 9485–9505.
12 N. Matsumi, K. Naka and Y. Chujo, *J. Am. Chem. Soc.*, 1998, **120**, 5112–5113.
13 S. Yamaguchi and K. Tamao, *Chem. Lett.*, 2005, **34**, 2–7.
14 S. Yamaguchi and A. Wakamiya, *Pure Appl. Chem.*, 2006, **78**, 1413–1424.
15 N. Matsumi and Y. Chujo, *Polym. J.*, 2008, **40**, 77–89.
16 F. Jäkle, *Chem. Rev.*, 2010, **110**, 3985–4022.
17 Y. Ren and F. Jäkle, *Dalton Trans.*, 2016, **45**, 13996–14007.
18 L. Ji, S. Griesbeck and T. B. Marder, *Chem. Sci.*, 2017, **8**, 846–863.
19 C. D. Entwistle and T. B. Marder, *Angew. Chem. Int. Ed.*, 2002, **41**, 2927–2931.
20 N. Matsumi, K. Naka and Y. Chujo, *J. Am. Chem. Soc.*, 1998, **120**, 10776–10777.

21 A. Sundararaman, M. Victor, R. Varughese and F. Jäkle, *J. Am. Chem. Soc.*, 2005, **127**, 13748–13749.
22 J. B. Heilmann, M. Scheibitz, Y. Qin, A. Sundararaman, F. Jäkle, T. Kretz, M. Bolte, H.-W. Lerner, M. C. Holthausen and M. Wagner, *Angew. Chem. Int. Ed.*, 2006, **45**, 920–925.
23 A. Lorbach, M. Bolte, H. Li, H.-W. Lerner, M. C. Holthausen, F. Jäkle and M. Wagner, *Angew. Chem. Int. Ed.*, 2009, **48**, 4584–4588.
24 D. Reitzenstein and C. Lambert, *Macromolecules*, 2009, **42**, 773–782.
25 F. Guo, X. Yin, F. Pammer, F. Cheng, D. Fernandez, R. A. Lalancette and F. Jäkle, *Macromolecules*, 2014, **47**, 7831–7841.
26 I. A. Adams and P. A. Rupar, *Macromol. Rapid Commun.*, 2015, **36**, 1336–1340.
27 A. Lik, L. Fritze, L. Müller and H. Helten, *J. Am. Chem. Soc.*, 2017, **139**, 5692–5695.
28 K. Hu, Z. Zhang, J. Burke and Y. Qin, *J. Am. Chem. Soc.*, 2017, **139**, 11004–11007.
29 X. Yin, J. Chen, R. A. Lalancette, T. B. Marder and F. Jäkle, *Angew. Chem. Int. Ed.*, 2014, **53**, 9761–9765.
30 Z. L. Zhang, R. M. Edkins, J. Nitsch, K. Fucke, A. Steffen, L. E. Longobardi, D. W. Stephan, C. Lambert and T. B. Marder, *Chem. Sci.*, 2015, **6**, 308–321.
31 X. Yin, F. Guo, R. A. Lalancette and F. Jäkle, *Macromolecules*, 2016, **49**, 537–546.
32 H. Li and F. Jäkle, *Macromol. Rapid Commun.*, 2010, **31**, 915–920.
33 P. Chen, A. S. Marshall, S.-H. Chi, X. Yin, J. W. Perry and F. Jäkle, *Chem. Eur. J.*, 2015, **50**, 18237–18247.
34 T.-Y. Chu, J. Lu, S. Beaupré, Y. Zhang, J.-R. Poulio, S. Wakim, J. Zhou, M. Leclerc, Z. Li, J. Ding and Y. Tao, *J. Am. Chem. Soc.*, 2011, **133**, 4250–4253.
35 J. Ohshita, Y.-M. Hwang, T. Mizumo, H. Yoshida, Y. Ooyama, Y. Harima and Y. Kunugi, *Organometallics*, 2011, **30**, 3233–3236.
36 C. M. Amb, S. Chen, K. R. Graham, J. Subbiah, C. E. Small, F. So and J. R. Reynolds, *J. Am. Chem. Soc.*, 2011, **133**, 10062–10065.
37 Y.-M. Hwang, J. Ohshita, Y. Harima, T. Mizumo, Y. Ooyama, Y. Morihara, T. Izawa, T. Sugioka and A. Fujita, *Polymer*, 2011, **52**, 3912–3916.
38 J. Ohshita, M. Miyazaki, D. Tanaka, Y. Morihara, Y. Fujita and Y. Kunugi, *Polym. Chem.*, 2013, **4**, 3116–3122.
39 J. Ohshita, M. Miyazaki, F.-B. Zhang, D. Tanaka and Y. Morihara, *Polym. J.*, 2013, **45**, 979–984.
40 D. Tanaka, J. Ohshita, Y. Ooyama and Y. Morihara, *Polym. J.*, 2013, **45**, 1153–1158.
41 F.-B. Zhang, J. Ohshita, M. Miyazaki, D. Tanaka and Y. Morihara, *Polym. J.*, 2014, **46**, 628–631.
42 J. Ohshita, M. Miyazaki, M. Nakashima, D. Tanaka, Y. Ooyama, T. Sasaki, Y. Kunugi and Y. Morihara, *RSC Adv.*, 2015, **5**, 12686–12691.
43 M. Nakashima, M. Miyazaki, Y. Ooyama, Y. Fujita, S. Murata, Y. Kunugi and J. Ohshita, *Polym. J.*, 2016, **48**, 645–651.
44 W. Ni, M. Li, F. Liu, X. Wan, H. Feng, B. Kan, Q. Zhang, H. Zhang and Y. Chen, *Chem. Mater.*, 2015, **27**, 6077−6084.
45 V. Gupta, L. F. Lai, R. Datt, S. Chand, A. J. Heeger, G. C. Bazan and S. P. Singh, *Chem. Commun.*, 2016, **52**, 8596–8599.
46 J. Ohshita, K.-H. Lee, D. Hamamoto, Y. Kunugi, J. Ikadai, Y.-W. Kwak and A. Kunai, *Chem. Lett.*, 2004, **33**, 892–893.
47 H. Usta, G. Lu, A. Facchetti and T. J. Marks, *J. Am. Chem. Soc.*, 2006, **128**, 9034–9035.
48 Z. Fei, J. S. Kim, J. Smith, E. B. Domingo, T. D. Anthopoulos, N. Stingelin, S. E. Watkins, J.-S. Kim and M. Heeney, *J. Mater. Chem.*, 2011, **21**, 16257–16263.
49 J. Shaw, H. Zhong, C. P. Yau, A. Casey, E. Buchaca-Domingo, N. Stingelin, D. Sparrowe, W. Mitchell and M. Heeney, *Macromolecules*, 2014, **47**, 8602−8610.
50 W. Zeng, Y. Cao, Y. Bai, Y. Wang, Y. Shi, M. Zhang, F. Wang, C. Pan and P. Wang, *Chem. Mater.*, 2010, **22**, 1915–1925.
51 S. Ko, H. Choi, M.-S. Kang, H. Hwang, H. Ji, J. Kim, J. Ko and Y. Kang, *J. Mater. Chem.*, 2010, **20**, 2391–2399.
52 L.-Y. Lin, C.-H. Tsai, K.-T. Wong, T.-W. Huang, L. Hsieh, S.-H. Liu, H.-W. Lin, C.-C. Wu, S.-H. Chou, S.-H. Chen and A.-I. Tsai, *J. Org. Chem.*, 2010, **75**, 4778–4785.
53 F. M. Jradi, X. Kang, D. O'Neil, G. Pajares, Y. A. Getmanenko, P. Szymanski, T. C. Parker, M. A. El-Sayed and S. R. Marder, *Chem. Mater.*, 2015, **27**, 2480−2487.
54 F. M. Jradi, D. O'Neil, X. Kang, J. Wong, P. Szymanski, T. C. Parker, H. L. Anderson, M. A. El-Sayed and S. R. Marder, *Chem. Mater.*, 2015, **27**, 6305−6313.
55 Y. Gao, X. Li, Y. Hu, Y. Fan, J. Yuan, N. Robertson, J. Hua and S. R. Marder, *J. Mater. Chem. A*, 2016, **4**, 12865−12877.
56 Y. Adachi, Y. Ooyama, N. Shibayama and J. Ohshita, *Dalton Trans.*, 2016, **45**, 13817−13826.
57 Y. Adachi, Y. Ooyama, N. Shibayama and J. Ohshita, *Chem Lett.*, 2017, **46**, 310−312.
58 A. Kunai, J. Ohshita, T. Iida, K. Kanehara, A. Adachi and K. Okita, *Synth. Met.*, 2003, **137**, 1007–1008.
59 T. Lee, I. Jung, K. H. Song, H. Lee, J. Choi, K. Lee, B. J. Lee, J. Pak, C. Lee, S. O. Kang and J. Ko, *Organometallics*, 2004, **23**, 5280–5285.
60 K.-H. Lee, J. Ohshita, K. Kimura, Y. Kunugi and A. Kunai, *J. Organomet. Chem.*, 2005, **690**, 333–337.
61 J. Ohshita, D. Hamamoto, K. Kimura and A. Kunai, *J. Organomet. Chem.*, 2005, **690**, 3027–3032.
62 J. Ohshita, K. Kimura, K.-H. Lee, A. Kunai, Y.-W. Kwak, E.-C. Son and Y. Kunugi, *J. Polym. Sci. A. Polym. Chem.*, 2007, **45**, 4588-4596.
63 J. Ohshita, Y. Kurushima, K.-H. Lee, A. Kunai, Y. Ooyama and Y. Harima, *Organometallics*, 2007, **26**, 6591–6595.
64 J. Ohshita, M. Nakamura, K. Yamamoto, S. Watase and K. Matsukawa, *Dalton Trans.*, 2015, **44**, 8214–8220.
65 J. Ohshita, Y. Adachi, D. Tanaka, M. Nakashima and Y. Ooyama, *RSC Adv.*, 2015, **5**, 36673–36679.
66 A. Meyer, E. Sigmund, F. Luppertz, G. Schnakenburg, I. Gadaczek, T. Bredow, S.-S. Jester and S. Höger, *Beilstein J. Org. Chem.*, 2010, **6**, 1180–1187.
67 N. Kitamura and E. Sakuda, *J. Phys. Chem. A*, 2005, **109**, 7429–7434.
68 Z. Zhang, R. M. Edkins, J. Nitsch, K. Fucke, A. Eichhorn, A. Steffen, Y. Wang and T. B. Marder, *Chem. Eur. J.*, 2015, **21**, 177–190.
69 M. Nakashima, Y. Ooyama, T. Sugiyama, H. Naito and J. Ohshita, *Molecules*, 2016, **21**, 789.
70 J. Hou, H.-Y. Chen, S. Zhang, G. Li and Y. Yang, *J. Am. Chem. Soc.*, 2008, **130**, 16144–16145.